INSIGHTS INTO THE DRIVEABILITY OF LARGE DIAMETER PILES

David Cathie, Cathie, Diegem, Belgium, David.Cathie@cathiegroup.com
Christophe Jaeck, Cathie, Diegem, Belgium, Christophe.Jaeck@cathiegroup.com
Erdem Ozsu, Cathie, Diegem, Belgium, Erdem.Ozsu@cathiegroup.com
Sylvie Raymackers, DEME Offshore, Zwijndrecht, Belgium, Raymackers.Sylvie@deme-group.com

ABSTRACT

Three large diameter (7.8m OD) monopiles were instrumented and monitored during driving with an IHC S-4000 hammer through more than 20m of stiff overconsolidated clay and into very dense sand. A detailed back analysis was performed to gain insights into the behaviour of large diameter piles during driving and to improve future pile driveability prediction methods. Signal matching using 1D wave equation modelling at 10 key penetrations was used to assess the SRD and calibrate the GRLWEAP model so that the measured hammer energy (ENTHRU) and blowcount could be used to develop a continuous SRD profile. Insights gained which are of importance for future driveability prediction of large diameter piles include limits on end bearing considered for the pile annulus in very dense sand, and shaft resistance and friction degradation in the clay.

Keywords: pile, driveability, signal matching, shaft resistance, end bearing, friction fatigue,

INTRODUCTION

Prediction of pile driveability remains largely empirical using simple 1-D wave propagation theory to represent the hammer-pile-soil interaction, and soil parameters derived mainly from pile driving back analysis (Alm and Hamre, 2001, 1998; Anusic et al., 2016; Byrne et al., 2012; Schneider and Harmon, 2010; Semple and Gemeinhardt, 1981).

As part of an R&D effort to improved driveability prediction for large diameter piles, Cathie Associates and Geosea (now DEME offshore) have been collaborating to develop a more fundamental understanding of their driving behaviour. Recently, Geosea installed the 7.8m base diameter monopiles at an offshore wind farm site through a formation of stiff clay and very dense sand. All piles drove through the sand layer without particularly high resistance. This behaviour has also been observed in pile installations in dense sand at other sites. Three piles were instrumented with pile dynamic monitoring (PDM) equipment by the Cathie company G-Octopus. A detailed analysis and extensive signal matching have been performed for one location to gain insights into the resistance of the very dense sand, the effect of interbedded sand and clay layers, and shaft resistance and friction fatigue in the clay. The results of this study are presented in this paper.

The 1D wave-equation does not account for the effects of radial inertia and radiation damping which are important for large diameter piles (see Deeks, 1992; Randolph and Deeks, 1992; Simons and Randolph, 1985). Therefore, signal matching using a 1D model can only capture the dominant parameters. It also has significant limitations when defining the distribution of shaft friction and end bearing. While the authors are aware of these limitations, we are also aware of the scarcity of measured pile driving data for large diameter piles in the public domain and the paucity of shaft resistance and end bearing data during driving for large diameter piles is even more acute than total resistance. For these reasons, the following results are presented as a contribution to understanding pile driveability without suggesting that they are more than indicative of actual behaviour.

SOIL CONDITIONS

The stratigraphic units relevant for the wind turbine foundations at the site under consideration are mostly Eocene deposits comprised of interbedded layers of sand and clay, deposited in an outer shelf to tidal flats environment. Soil conditions relevant to the present study are summarized in Table 1 and CPT data in Figure 1. Soil parameters are given as mean values for the formation or location where available, or typical values where data is limited. The water depth was approximately 30m.

Table 1. Soil properties

Parameter	Clay A	Clay B	Sand
Depth BSF [m]	3.5 - 18	18 - 27	27 – 36
Description	Fissured firm to hard silty slightly micaceous CLAY	Stiff to hard sandy silty CLAY	Silty clayey fine to medium SAND
Bulk density [Mg/m^3]	1.93	2.10	2.01
Water content [%]	34	24	27
Plasticity index [%]	92	27	-
Particle size, d_{10} [mm]			~0.006-0.06
Cone resistance, q_c [MPa] (depth, z in m)	1+0.1z (4<z<18)	see Fig. 1	>100
Cone sleeve friction, f_s [kPa] (depth, z in m)	60+5z (4<z<16)	see Fig. 1	>750
Undrained strength (UU) [kPa]	178	151	-
Relative density [%]	-	-	~100
Peak friction angle [°]	-	-	38
Remoulded strength [kPa]	166	85	-
Residual friction angle [°]	9°	21°	31°
G_{max} P-S logging [MPa]	100-200	180-320	200-600

The sand formation is a silty clayey fine and medium SAND with frequent to abundant fine to medium gravel sized shell fragments and rare intact shells. The formation contains minor sublayers of sandy clayey SILT and stiff to very stiff dark fissured CLAY. Parts of the layer are described as silty slightly clayey and parts contain occasional sand sized mica crystals. Particle size distributions indicate between 10 – 23% of fines (silt and clay) with a mean of 17%. There was no evidence of cementation in the samples recovered. The “flat line” CPT traces are characteristic of the formation across the site and are also characterized by negative excess pore pressures limited by cavitation. In-situ pressuremeter tests closest to the study location indicated a K_0 of approximately 2.0 in Clay A although values up to 3.7 were recorded across the site. This could mean that similar high lateral stresses are also present in the sand layer and contribute to the very high cone resistance.

PILE AND HAMMER CHARACTERISTICS

The studied monopile was a tapered design with 5.6m diameter (*D*) in the top section and 7.8m diameter in the bottom section. The tapered section between the two constant sections was 24.2m long and the total pile length 76.6m. Wall thickness (*t*) varied between 65 - 85mm. At the lower end of the bottom section, a 2m “shoe” with 78mm wall thickness (annulus area

1.89m^2) was present. The piles were driven with an IHC S-4000 hammer which has a maximum rated energy of 4000kJ, a ram weight of 1977kN and an anvil weight of 2256kN.

PILE DRIVING

Driving took 1h:30min with blowcount and hammer energy data as shown on Figure 1. The total number of blows was 3519, and between 29 and 42m the average blow rate was 38 blows/minute (1.56 seconds/blow) and the average set was 8.6mm.

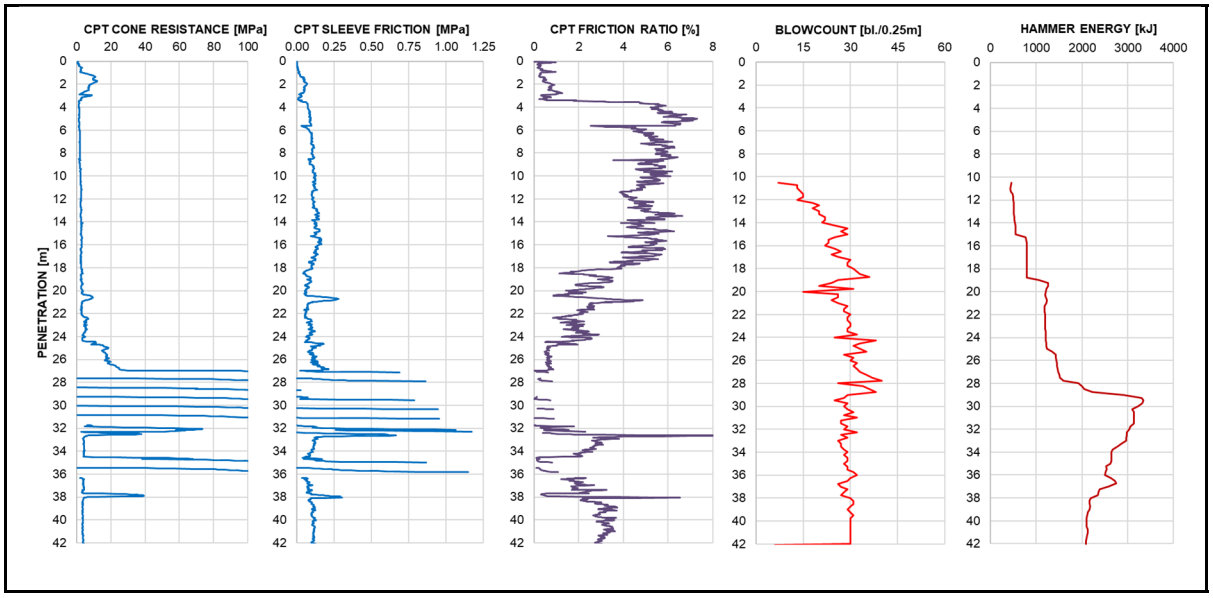

Fig. 1. Site CPT data, measured blowcount and hammer energy

MONITORING AND SIGNAL MATCHING

Instrumentation

The instrumented section was at 11.2m from the MP top (approximately in the centre of the tapered section), with 4 strain transducers and 2 piezo-resistive accelerometers bolted on supports welded to the MP shaft. A correction of the strain signals was required to account for the geometry of the supports and a small correction on the accelerometer signals to account for the signal cable length. These corrections improve the force and velocity proportionality.

Signal matching

An initial estimate of the shaft resistance distribution and shaft resistance/end bearing split for each blow analysed was calculated based on Alm and Hamre, (2001) referred to as the A&H method subsequently. These distributions were used as the starting point for the signal matching process to constrain the shaft resistance distributions to physical reality. The signal matching proceeded by setting initial parameters to standard values (quake: 2.5mm, shaft damping: 0.25 s/m, toe damping: 0.5 s/m) with no radiation damping. The shaft friction was then iteratively adjusted in order to match the signal. Once the initial stage of the signal matching was complete, radiation damping was introduced to improve the visual match quality and the least squares-based match quality index. Unit shaft resistances reported in this paper are assumed to apply on the inside and outside of the pile and be of equal magnitude. The interpreted SRDs from the signal matching performed at different depths are shown on Figure 2.

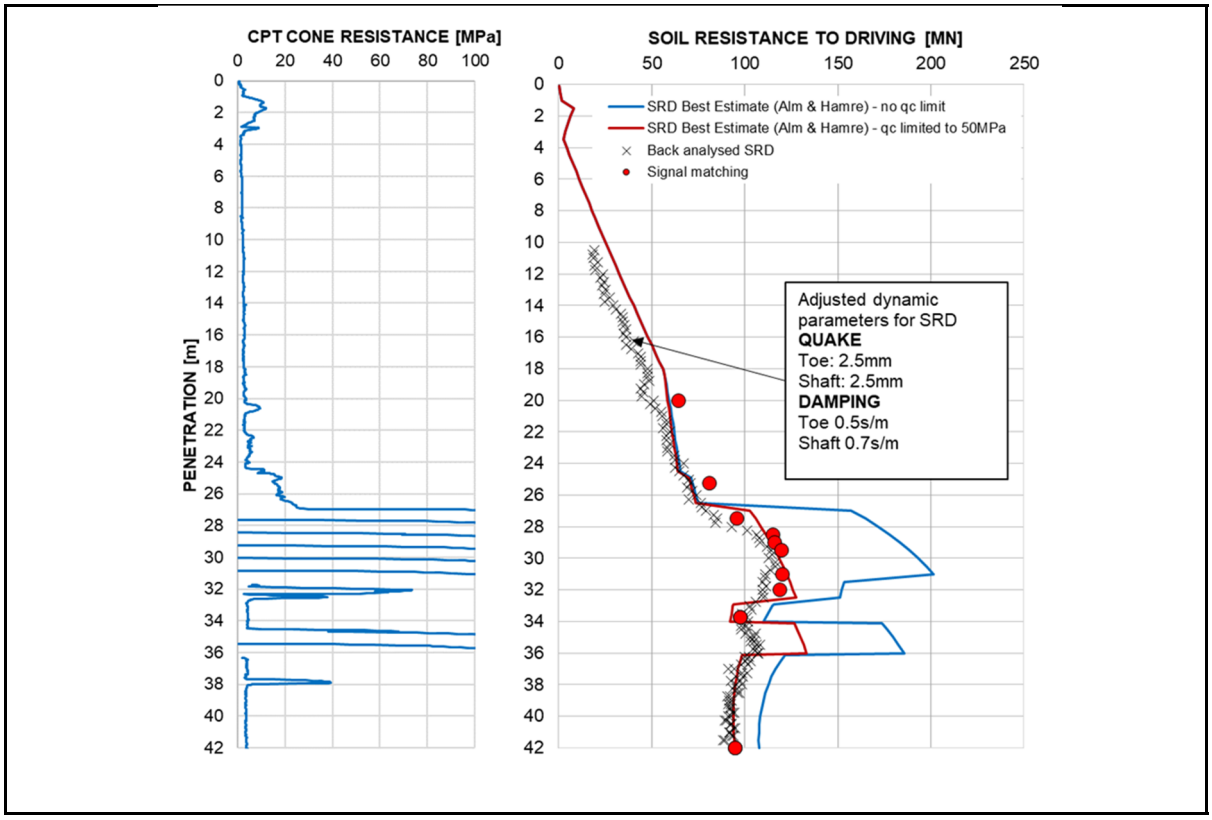

Fig. 2. Interpreted SRD from signal matching and calibrated wave equation method

Back-analysis using global SRD method

A GRLWEAP model of the pile and soil resistance was then calibrated to the results of the signal matching using the recorded hammer energy and blow counts indicated as "back analysed SRD" in Figure 2. Calibration was performed to obtain a good match with the pile resistance at 42m. A Smith shaft damping of 0.7s/m was needed to match the signal matching results at end of drive. Slightly lower shaft damping would be needed to accurately match the results in the clay and sand above about 32m. However, the overall consistency of the signal matching and the global method is reasonable. The high damping compared to standard values used for smaller piles is believed to be required to compensate for the lack of radiation damping in the GRLWEAP model.

ANALYSIS OF RESULTS

Predicted and measured SRD

An SRD calculation for the site and pile using the A&H method (best estimate) for two cases: a) without a cone resistance limit and b) with a limit of 50MPa is also shown on Figure 2 (the limit affecting both the end bearing and shaft resistance). Note that no embedment effects which could reduce the end bearing resistance in the sand layer have been applied as per normal practice for conservative pile driving predictions.

Overall, the A&H SRD calculation method provides a reasonable fit to these data in both clay and sand provided a (rather arbitrary) cone resistance limit of 50MPa is applied. However, it is important to note that the standard A&H method was calibrated using a shaft damping value of 0.25 s/m in the wave equation modelling (Alm and Hamre, 2001, 1998) while the back calculated SRD based on signal matching is associated with a higher damping.

By inspection of Figure 2, at approximately 28.5m penetration, when the pile tip is approximately 1m into very dense sand a total resistance increase on the order of 25MN may be estimated. Some further increase in total resistance occurs over the next 2m but the increase is much more limited. This seems to indicate that the end bearing is approximately constant once the embedment into the sand layer has reached about 1.5m (i.e.19*t*, where *t* is the wall thickness). The sudden drop in resistance between 32 and 34m seems to confirm that much of the 25MN is annulus resistance. If this is the case, the unit end bearing is 13.2MPa.

The maximum resistance is observed at 30m depth. By the time the pile reaches 34m penetration, the end bearing component from the sand has been lost and the frictional resistance of the sand layer is substantially reduced and of a similar magnitude to the clay above. The SRD is hardly affected by the thin dense sand layer between 34.5 – 36.0m which only mobilises a small fraction of the end bearing observed in the thicker layer above.

End bearing in sand

General Observations:

The unit end bearing applicable during pile driving has not been studied to the same extent as end bearing resistance under static loading although many of the same considerations apply (see for example Schneider et al., 2010; Schneider and Harmon, 2010). Based on strain measurements during penetration, White (2002) showed that for drained penetration in sand significant grain crushing and particle breakage occurs just below the pile tip in a “nose cone” with zones of vertical compression/horizontal extension, horizontal compression/vertical extension and dilation as shown in Figure 3. Rapid loading tests of piles in sand in a centrifuge by Hölscher et al. (2012) confirm the different zones of contraction and dilation as measured by the excess pore pressure response either positive or negative (suction). The pore pressure response was also dependent on the partial dissipation which occurs during the rapid loading test.

While there is general agreement that the cone penetration resistance provides a good basis to predict pile end bearing resistance for static capacity assessment, the differences of scale must be considered (see White, 2002, for a summary of these corrections). This is often addressed by averaging the cone resistance above and below the pile, and ensuring the minimum resistance in the zone is considered (Schmertmann, 1978; Tomlinson and Woodward, 2005; Gavin et al (2019). One required correction when using CPT data for driveability studies is the pile embedment depth into the stronger layer and whether a weaker layer below is influencing the resistance (De Beer, 1971). In dense sand, a “critical depth” to achieve “quasi-stationary” penetration resistance is between 10 – 20 times the governing dimension – either the cone diameter, or the pile diameter for closed or plugged piles (Meyerhof, 1951; Puech and Foray, 2002). For unplugged piles, the pile wall thickness at the tip may be considered the relevant dimension.

Considering a pile wall thickness (*t*) of 78mm at the tip, the full end bearing resistance would require between 1 and 2m penetration to develop due to embedment effects. This is consistent with the installation experience when entering or leaving the main sand layer (27-32m) and the limited resistance between 34.5-36m. However, it does not explain the full reduction in end bearing in the main sand layer which is now discussed.

Undrained interpretation:

One CIU triaxial test for the sand at the site was performed at 28m depth and revealed an undrained strength at 10% strain of 462kPa for a sample relative density of 84%. Undrained cyclic loading at 60% of the static shear resistance followed by post-cyclic shearing indicated no significant change in strength but pore water cavitation was observed which would limit the shearing resistance. A DSS test at a similar depth in the same formation indicated an undrained

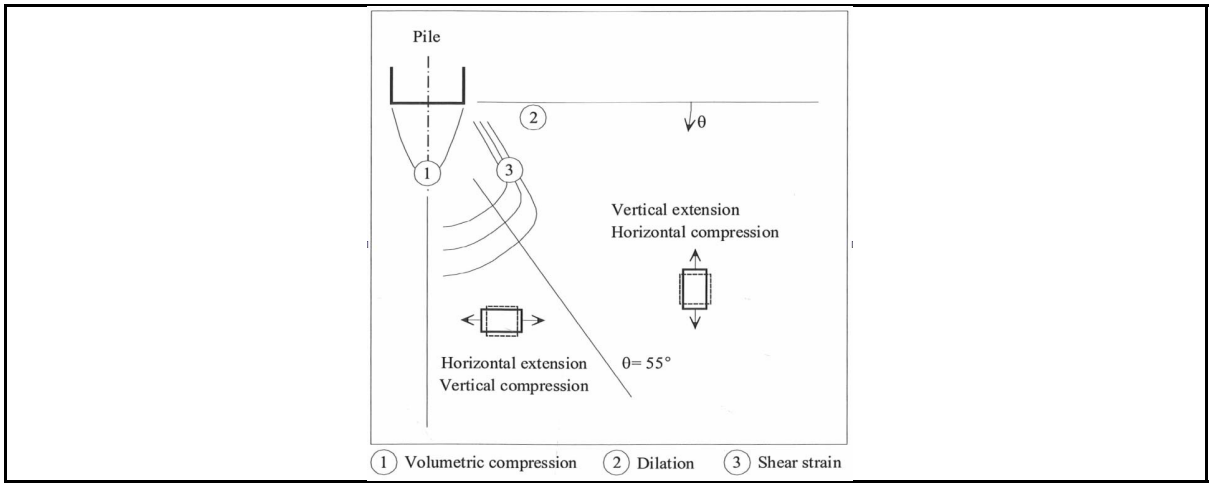

Fig. 3. Generalised pattern of strain during an increment of drained penetration (White, 2002)

strength of 380kPa. These results are therefore believed to underestimate the in-situ strength of the sand.

Andersen (2015) provides data for the undrained triaxial shear strength of very dense silty sand indicating s_u/σ'_{ref} ~10 at 5% strain (for relative density 90-100%). At 30m depth, this corresponds to an undrained strength of 1730kPa (s_u/σ'_{vc} ~ 6). Other data in the same paper indicate s_u/σ'_{vc} ~ 10 in triaxial compression (i.e. s_{uTC} = 3000kPa for Dogger bank sand, Table 10.1) but s_u/σ'_{vc} ~ 2 – 3 in DSS and triaxial extension with high fines content (i.e. s_{uDSS} = 600 – 900kPa).

Assuming initially that the full 25MN at 28.5m is annulus resistance, the equivalent bearing pressure 13.2MPa. The pile velocity during penetration is such that conditions are essentially undrained and therefore an equivalent undrained strength may be estimated. Adopting a bearing capacity factor N_c=7.5 for an embedded strip footing, the equivalent undrained shear strength is 13.2/7.5*1000 = 1760kPa and assuming σ_{v0}'at this depth is 300kPa it leads to s_u/σ_{v0}' ~ 6. If part of the 25MN total resistance were shaft friction, the equivalent undrained strength would be reduced. Application of the A&H method for q_c limited to 50MPa, gives an initial radial stress of 380kPa and unit shaft friction of 200kPa. Considering an embedment of 1.5m produces a shaft resistance of 14.6MN ignoring embedment depth effects and an annulus bearing of 10.4MN. This leads to a low estimate equivalent undrained strength of 732kPa (s_u/σ_{v0}' ~ 2.4).

Overall, the working shear strength of the sand layer based on the dynamic monitoring and signal matching is thus estimated to be between 700 – 1700 kPa. This interpreted range is reasonably consistent with published data for silty sands considering that the average strength (compression, simple shear, extension) would be appropriate. Consideration of the pore pressure response during driving allows this range to be constrained.

Pore pressure response during driving - cavitation

Limits to the negative excess pore water pressures and therefore the short-term peak effective stresses which can develop during driving result from pore water cavitation. Cavitation occurs when the absolute pressure in the water drops below the vapour pressure. At 30m penetration in 30m water depth, the vapour (or cavitation) pressure is the hydrostatic pressure plus atmospheric pressure i.e. 700kPa. This establishes an approximate limit on the effective stress at failure of about 1000kPa (700kPa plus the initial vertical effective stress of 300kPa). Assuming a peak friction angle of 38° (see Table 1), a limiting shearing resistance of 780kPa is indicated if cavitation occurs.

Pore pressure accumulation and redistribution

Measurements of the permeability or consolidation characteristics of the sand layer were not made but drainage was sufficiently slow during the CPT testing that the pore pressure sensor consistently reached the cavitation limit in the top of the sand layer at about 26m (660kPa). Based on the grain size distribution of this clayey, silty fine to medium sand a permeability in the range 10^{-6} – 10^{-7}m/s is indicated leading to a characteristic drainage time, $T = t^2/c_v$, of between 0.4 – 4s. Since the average blow period was 1.56s, excess pore pressures will not be fully dissipated between blows around the pile tip. Immediately below and around the pile tip the strain field is highly variable (White, 2002) and areas of contraction and dilation are likely to occur (see also Hölscher et al., 2012). Extremely high pore pressure gradients and therefore changes in effective stress will be developed for very short periods as the compression wave reaches the pile toe and causes penetration. The effect of repeated intense cyclic loading during driving, the strong rotation of principal stress/strain direction as the pile and soil move relatively to each other, the additional local effect of pore pressure gradients, and particle breakage are all likely to lead to increased pore water pressures and therefore contribute to limiting the working shear strength.

Conclusion on end bearing in the sand layer

Annulus end bearing develops within about 20 wall thicknesses (1.5m) of the tip encountering the sand layer and starts to be lost again at about the same distance above a weaker layer. Based on the signal matching and considerations of pore pressure accumulation and cavitation, a working undrained shear strength of 800 – 1000kPa is estimated for this layer. This corresponds to a unit end bearing on the annulus of only 6 – 7.5MPa despite the high cone resistance.

Shaft resistance during driving

The signal matching performed at different pile penetrations also provides a unique opportunity to study the shaft friction during driving. The reliability of shaft resistance distribution deduced from signal matching is much lower than for the total driving resistance (SRD). However, when anchored to physical reality, reliable qualitative trends are expected. Figure 4 shows the evolution of the shaft resistance for pile penetrations between 20 and 32m. As the pile tip enters the very dense sand at 27m and builds up resistance, it becomes more difficult to distinguish the end bearing component from the shaft resistance near the pile tip and some scatter develops. However, the overall trend of reducing shaft friction with penetration, i.e. friction degradation, is very clear.

Degradation of the shaft resistance at a given depth below seabed as the pile progressively passes that level has been calculated from the unit shaft resistance profiles (shown in Figure 4) and are presented on Figure 5. For example, at 10m depth, the unit shaft resistance is 57kPa when the pile tip is at 20m penetration (10m relative movement) reducing to about 26kPa when the tip is at 32m (22m relative movement). Also shown are the A&H initial unit shaft resistance (based on the CPT sleeve friction) and the degradation with relative displacement at 20m and 25m depth below seabed.

The back calculated unit shaft resistance is approximately 25% higher than indicated by the A&H model but the observed degradation occurs more rapidly at the study site. Normalising the reducing shaft resistance (f_s) with the initial unit resistance (f_{si}) observed as the pile tip passes that level reveals the more rapid degradation experienced by the large diameter pile compared to the A&H degradation model (Figure 6).

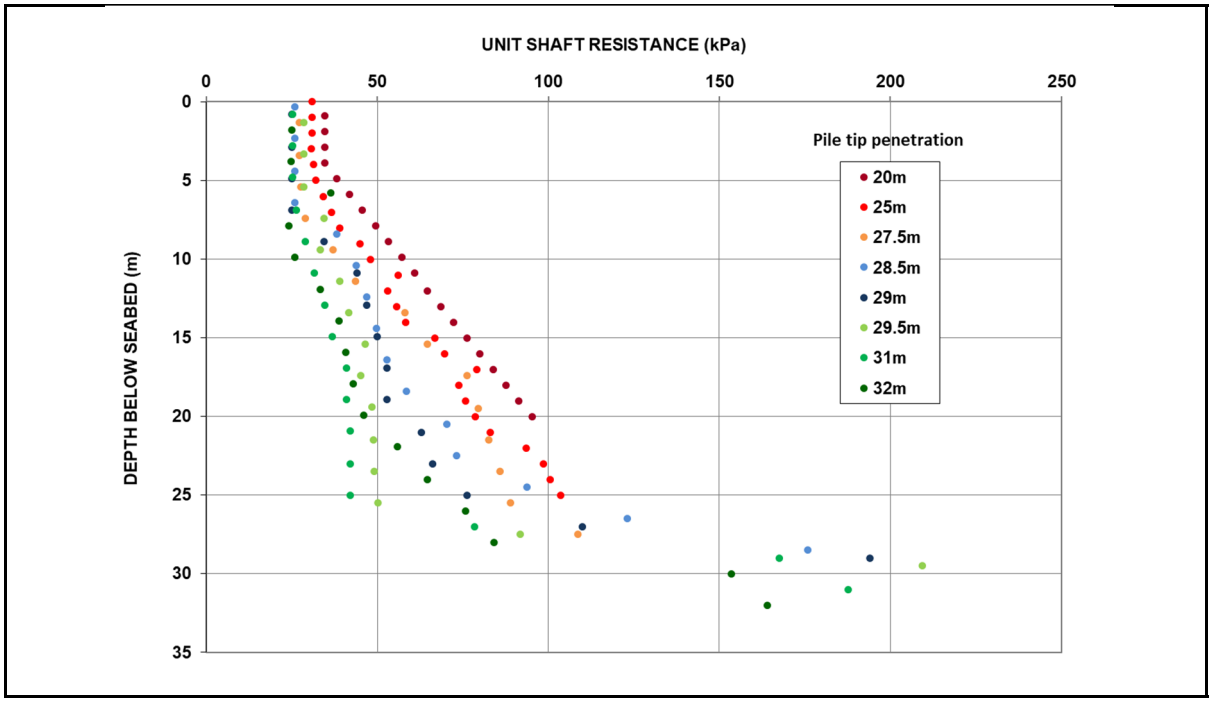

Fig. 4. Unit shaft resistance at different pile penetrations from signal matching

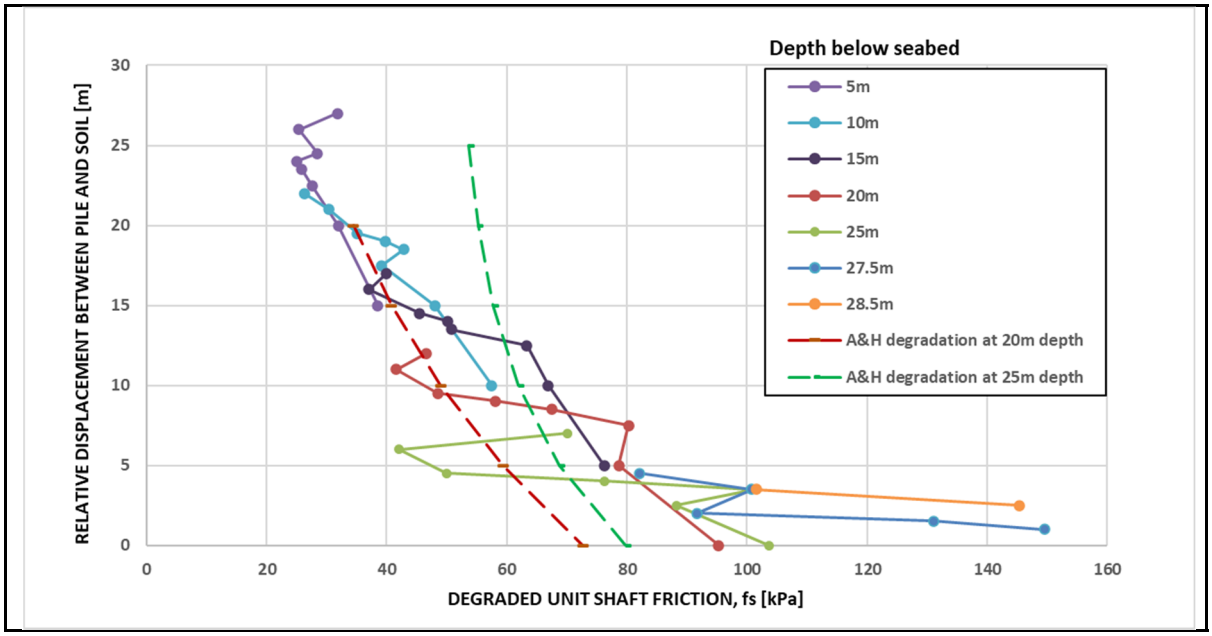

Fig. 5. Degradation of unit shaft resistance with relative displacement

The combination of underestimating the initial friction and underestimating the rate of degradation results, perhaps fortuitously, in a reasonable match. In the case studied in this paper, the residual unit resistance does not appear to have been achieved within 20m of relative movement. Finally, it is noted that the A&H model is calibrated based on a lower damping than is found necessary to match the PDM signals and care needs to be used to transpose these conclusions to other projects and predictions. The more aggressive friction degradation for the large piles is attributed primarily to the large radial expansion which is proportional to the pile diameter (for the same axial stress). In the present example, when driving at 30m penetration the maximum radial expansion at mudline calculated from the maximum axial stress/strain is approximately 0.7mm.

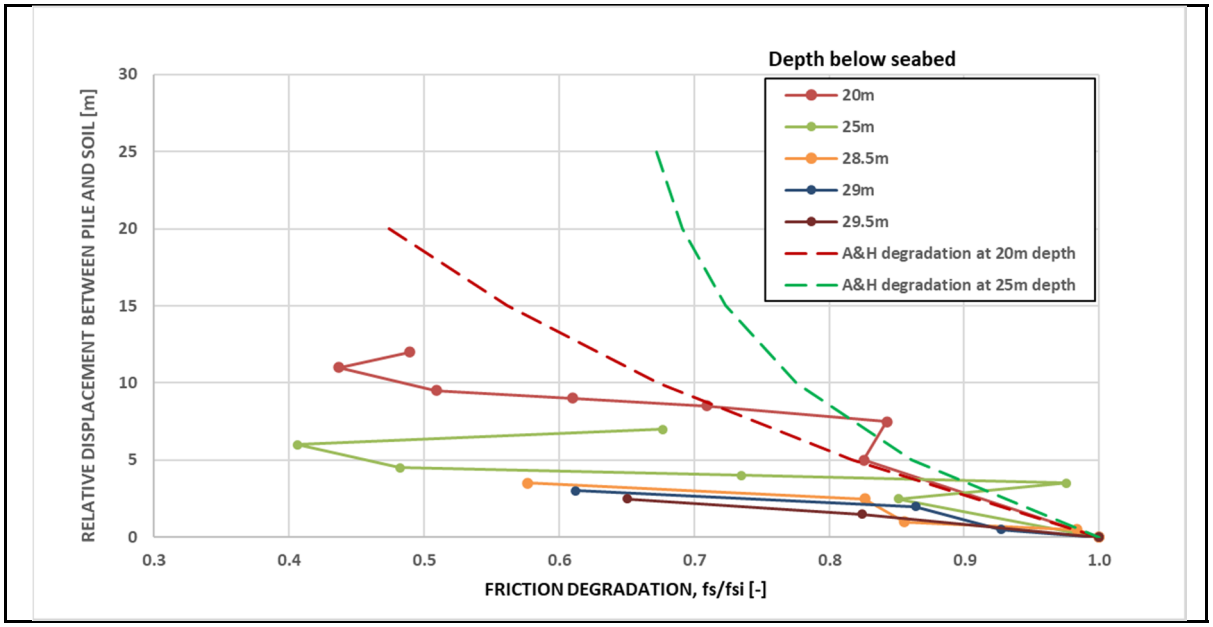

Fig. 6. Normalised degradation of unit shaft resistance with relative displacement

A small tensile wave is also reflected from the pile tip, so a small radial contraction also occurs shortly afterwards. It is also possible, but more speculative, that the friction degradation is affected by the relatively flexible monopile (max *D/t*=120 in the lower embedded section).

SUMMARY AND CONCLUSIONS

A detailed back analysis of a large diameter pile driven into stiff to hard clay and very dense sand has provided the following insights:

1) Driving through the sand (q_c > 100MPa) was much easier than predicted by standard SRD methods. While the reasons for the relatively low driving resistance remain speculative, this study shows that possible explanations include a) pore water cavitation limiting the shearing resistance during rapid pile tip penetration, b) accumulation of pore water pressures in the area of the pile toe due to repeated blows, and c) very high local hydraulic gradients around the pile tip during a blow. A unit end bearing of between 6 – 7.5MPa corresponding to a working undrained strength on the order of 800-1000kPa was estimated.

2) A penetration of approximately 1.5m (20 wall thicknesses) was required to reach a quasi-steady state penetration resistance and the effect of a weaker layer below was felt at about the same distance above the layer. Therefore, smoothing/scaling methods to account for these effects should be used for driveability studies as they are for pile design.

3) Friction fatigue was observed to occur more rapidly in the clay formations compared to the standard A&H SRD method but the initial shaft friction was also underestimated by this method. Therefore, the overall shaft friction in the clay was reasonably matched if a higher shaft damping (e.g. 0.7s/m) is used for the wave equation modelling to account for radiation damping.

ACKNOWLEDGEMENTS

The authors wish to acknowledge the work of Chiara Prearo and Fabrizio Calidonna of Cathie who performed the signal matching for this study.

REFERENCES

Alm, T., Hamre, L., 2001. Soil model for pile driveability predictions based on CPT interpretations. Presented at the International Conference On Soil Mechanics and Foundation Engineering.

Alm, T., Hamre, L., 1998. Soil model for driveability predictions. Presented at the OTC 8835, Annual Offshore Technology Conference, Houston, Texas, p. 13.

Andersen, K.H., 2015. Cyclic soil parameters for offshore foundation design, in: 3rd ISSMGE McClelland Lecture. Presented at the ISFOG.

Anusic, I., Eiksund, G.R., Liingaard, M.A., 2016. Comparison of pile driveability methods based on a case study from an offshore wind farm in North Sea, in: Proceedings of the 17th Nordic Geotechnical Meeting. Reykjavik, pp. 1037–1046.

Byrne, T., Doherty, P., Gavin, K., Overy, R., 2012. Comparison of Pile Driveability Methods in North Sea Sand. 7th Int. Conf. Offshore Site Investigation and Geotechnics, SUT, pp. 481–488.

De Beer, E, 1971. Methodes de deduction de la capacite portante d'un pieu a partir des resultats des essais de penetration.

Deeks, A.J., 1992. Numerical analysis of pile driving dynamics. University of Western Australia.

Gavin, K, Kovacevic, M.S. and Igoe, D., 2019 A review of CPT based axial pile design in the Netherlands, ScienceDirect, https://doi.org/10.1016/j.undsp.2019.09.004

Hölscher, P., van Tol, A.F., Huy, N.Q., 2012. Rapid pile load tests in the geotechnical centrifuge. 9th International Conference on Testing and Design Methods for Deep Foundations 52, 1102–1117. https://doi.org/10.1016/j.sandf.2012.11.024

Meyerhof, G.G., 1951. The ultimate bearing capacity of foundations. Geotechnique 2, 301–332.

Puech, A., Foray, P., 2002. Refined Model for Interpreting Shallow Penetration CPTs in Sands. Presented at the Offshore Technology Conference, Houston, Texas.

Randolph, M.F., Deeks, A.J., 1992. Dynamic and static soil models for axial pile response, in: 4th Int. Conf. on the Application of Stress-Wave Theory to Piles. The Hague, pp. 3–14.

Schmertmann, J.H., 1978. Guidelines for Cone Penetration Test - Performance and Design.

Schneider, J.A., Harmon, I.A., 2010. Analyzing drivability of open ended piles in very dense sands. J. Deep Found. Inst. 4, 32–44.

Schneider, J.A., Xu, X., Lehane, B.M., 2010. End bearing formulation for CPT based driven pile design methods in siliceous sands. 2nd Int. Symp. on Cone Penetration Testing, Huntington Beach, CA, USA, p. 8.

Semple, R.M., Gemeinhardt, J.P., 1981. Stress History Approach to Analysis of Soil Resistance to Pile Driving, OTC 3969, Offshore Technology Conference, pp. 165–169.

Simons, H.A., Randolph, M.F., 1985. A new approach to one dimensional pile driving analysis. Proc. 5th Int. Conf. on Numerical Methods in Geomechanics.

Tomlinson, M.J., Woodward, J., 2005. Pile design and construction practice - 6th edition.

White, D.J., 2002. An investigation into the behaviour of pressed-in piles, PhD Thesis, University of Cambridge.